THE HENRYK NIEWODNICZAŃSKI
INSTITUTE OF NUCLEAR PHYSICS
POLISH ACADEMY OF SCIENCES

Exploring spin and structural correlations in molecular and frustrated magnets

Prospects of next-generation neutron scattering

dr. rer. nat. Naveen Kumar CHOGONDAHALLI MUNIRAJU

Institute of Molecular Magnetism (NZ37)
The Henryk Niewodniczański Institute of Nuclear Physics, Polish Academy of Sciences, Kraków, Poland

1st Workshop on Research & Innovation in Poland, Dec 01-02, 2025

Functional PBA magnets – examples & possible applications

What are PBAs?

Cyano-bridged, open-framework compounds: $AM[P(CN)_6]\cdot nH_2O$

A = Alkali or ammonium cation (K^+, Rb^+, Cs^+, NH_4^+)

M[P(CN)6] = Two transition-metal (M, P) sites bridged by cyanide

Mixed-valence & flexible lattice → valence, spin, *and* structural switching

- **External triggers: Temperature**, pressure, light, humidity, E-field
- **Several degrees of freedom to tune functionality:** Tune metal ions, A-site cations, vacancies, hydration etc.
- Room-temperature magnetism, photomagnetism, barocaloric and magnetocaloric effects, etc.

Magnetic thermal hysteresis of Charge-Transfer transition

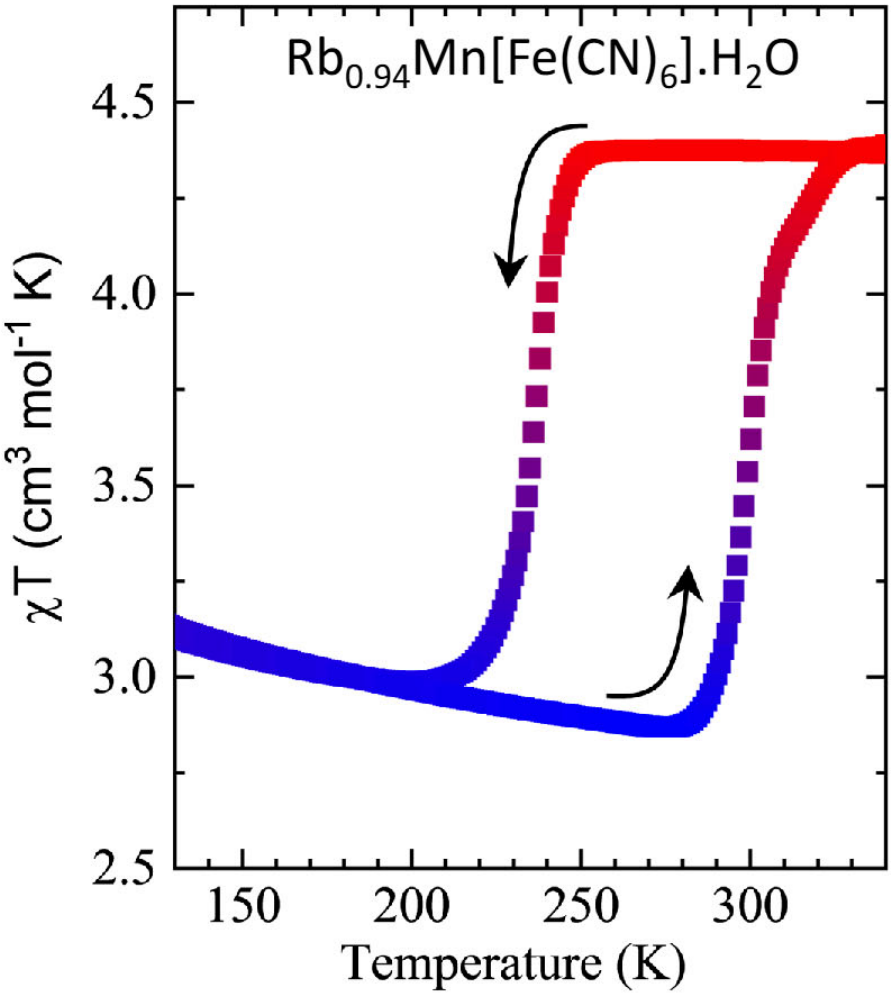

Magnetic thermal hysteresis of Charge-Transfer transition

Ion	Spin State	Unpaired electrons	$\chi_{M^*}T$ $cm^3 \cdot mol^{-1} \cdot K$
Mn^{2+}	HS	5	4.375
Fe^{3+}	LS	1	0.375
Mn^{2+}	LS	1	0.375
Fe^{3+}	HS	5	4.375
Mn^{3+}	HS	4	3.00
Fe^{2+}	LS	0	0.00
Mn^{3+}	LS	2	1.00
Fe^{2+}	HS	4	3.00

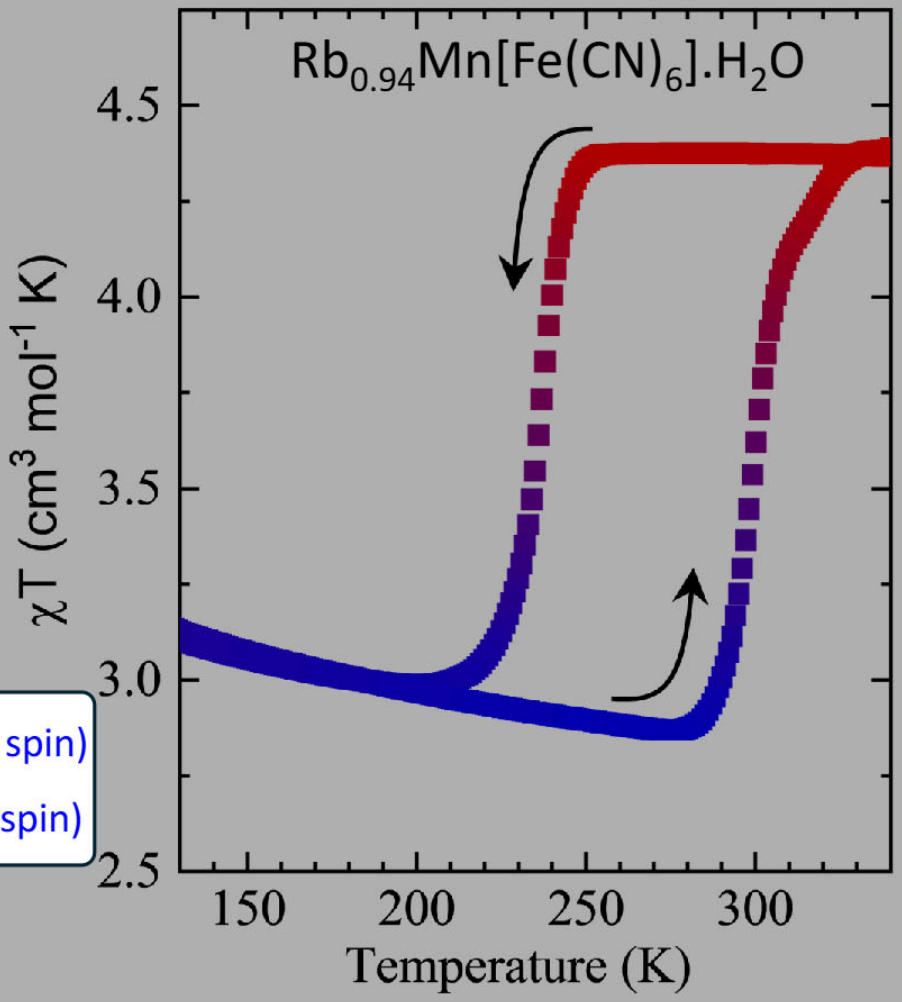

Mn^{II} $(d^5) \rightarrow s = \frac{5}{2}$ (High spin)

Fe^{III} $(d^5) \rightarrow s = \frac{1}{2}$ (Low spin)

Mn^{III} $(d^4) \rightarrow s = 2$ (High spin)

Fe^{II} $(d^6) \rightarrow s = 0$ (Low spin)

Magnetic thermal hysteresis of Charge-Transfer transition

Ion	Spin State	Unpaired electrons	$\chi_{M^*}T$ $cm^3 \cdot mol^{-1} \cdot K$
Mn^{2+}	HS	5	4.375
Fe^{3+}	LS	1	0.375
Mn^{2+}	LS	1	0.375
Fe^{3+}	HS	5	4.375
Mn^{3+}	HS	4	3.00
Fe^{2+}	LS	0	0.00
Mn^{3+}	LS	2	1.00
Fe^{2+}	HS	4	3.00

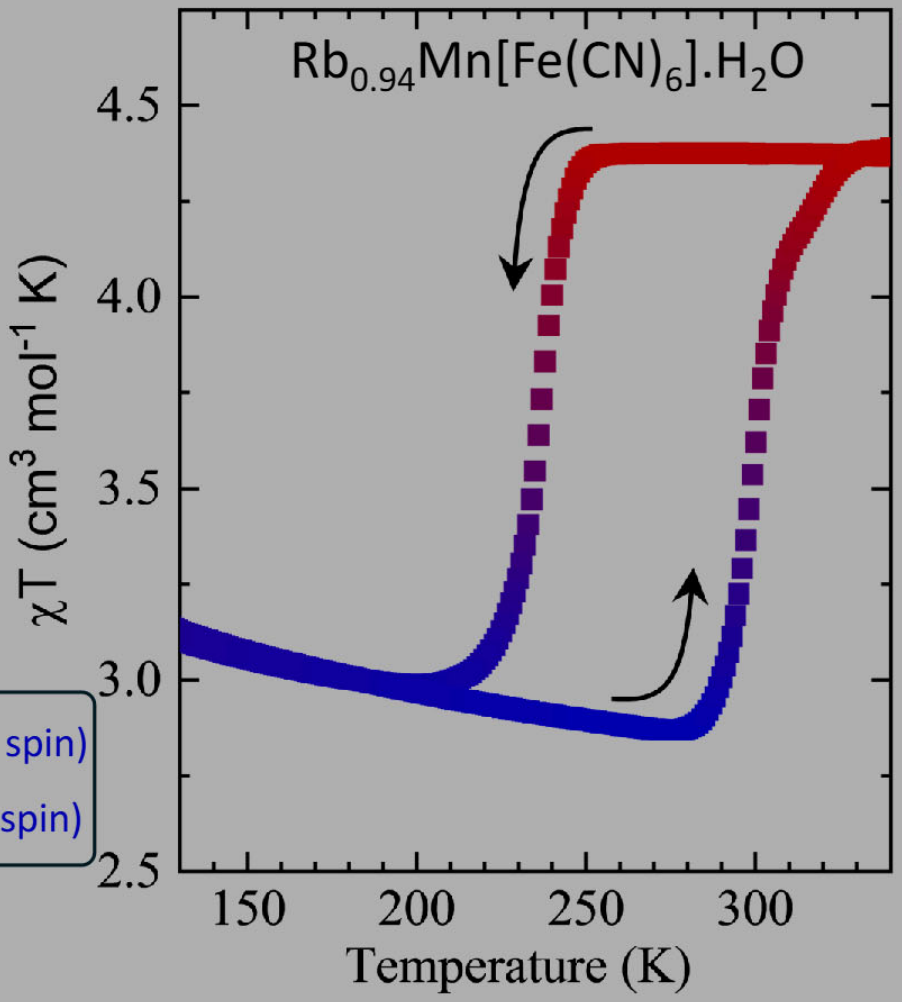

Mn^{II} $(d^5) \rightarrow s = \frac{5}{2}$ (High spin)

Fe^{III} $(d^5) \rightarrow s = \frac{1}{2}$ (Low spin)

Mn^{III} $(d^4) \rightarrow s = 2$ (High spin)

Fe^{II} $(d^6) \rightarrow s = 0$ (Low spin)

Ion	State	JT Active?
Mn^{2+} (HS)	$d^5\ (t_{2g}^3 e_g^2)$	No
Fe^{3+} (LS)	$d^5\ (t_{2g}^5 e_g^0)$	No
Mn^{3+} (HS)	$d^4 (t_{2g}^3 e_g^1)$	Yes (strong)!
Fe^{2+} (LS)	$d^6 (t_{2g}^6 e_g^0)$	No

Evolution of structure across Charge-transfer transition temperature

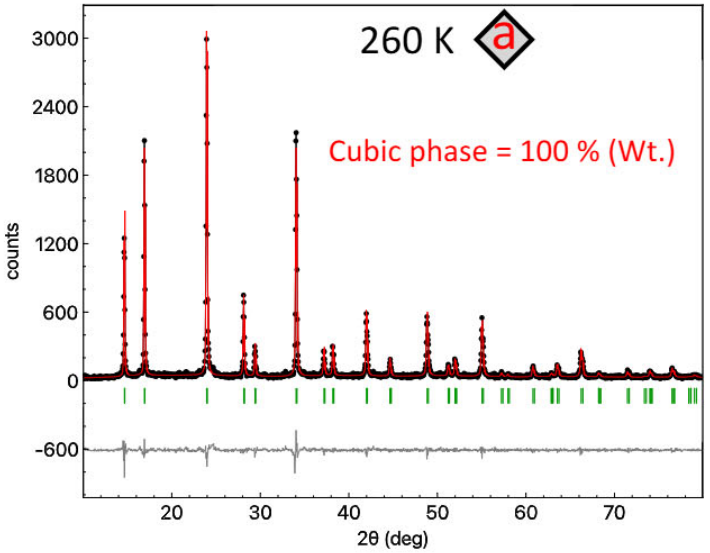

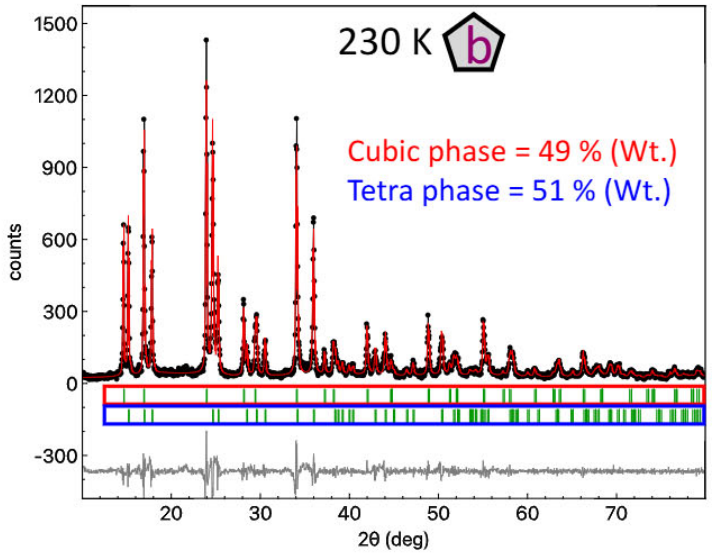

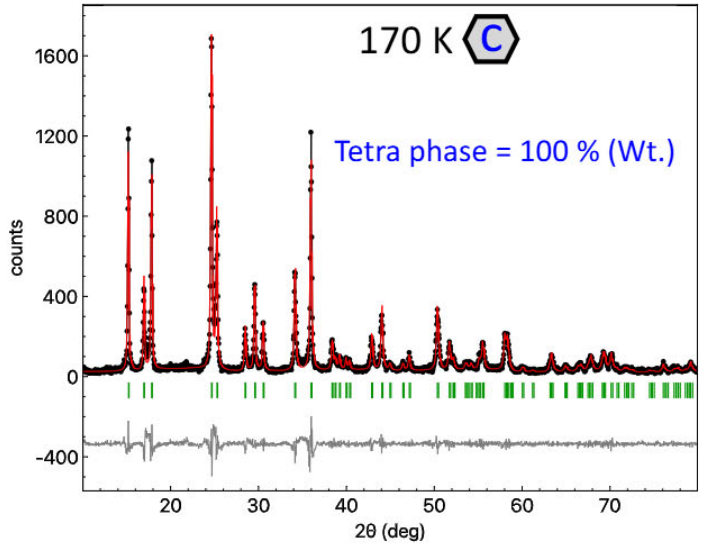

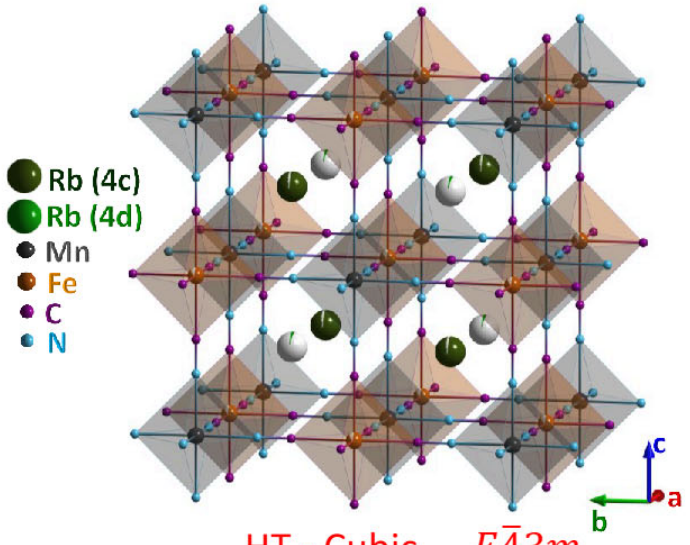

HT - Cubic $F\bar{4}3m$

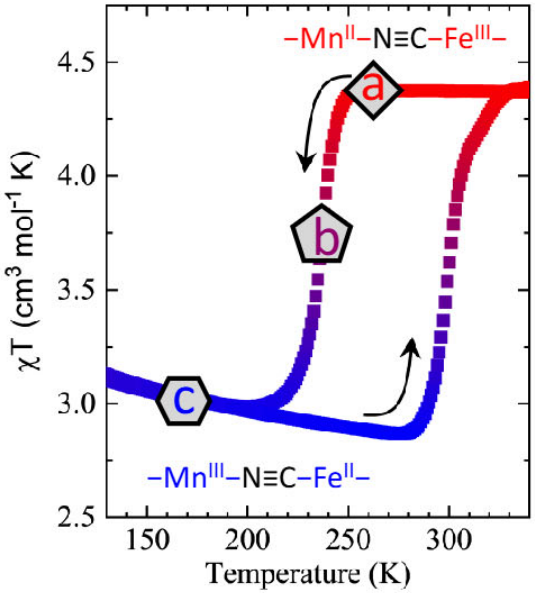

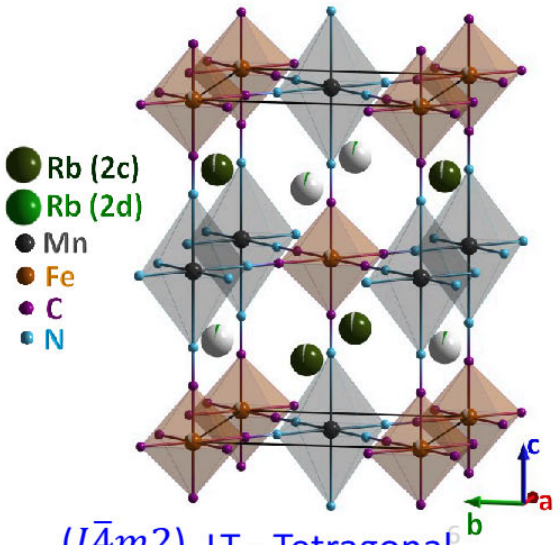

$(I\bar{4}m2)$ LT - Tetragonal

Coupled electronic and structural bistabilities

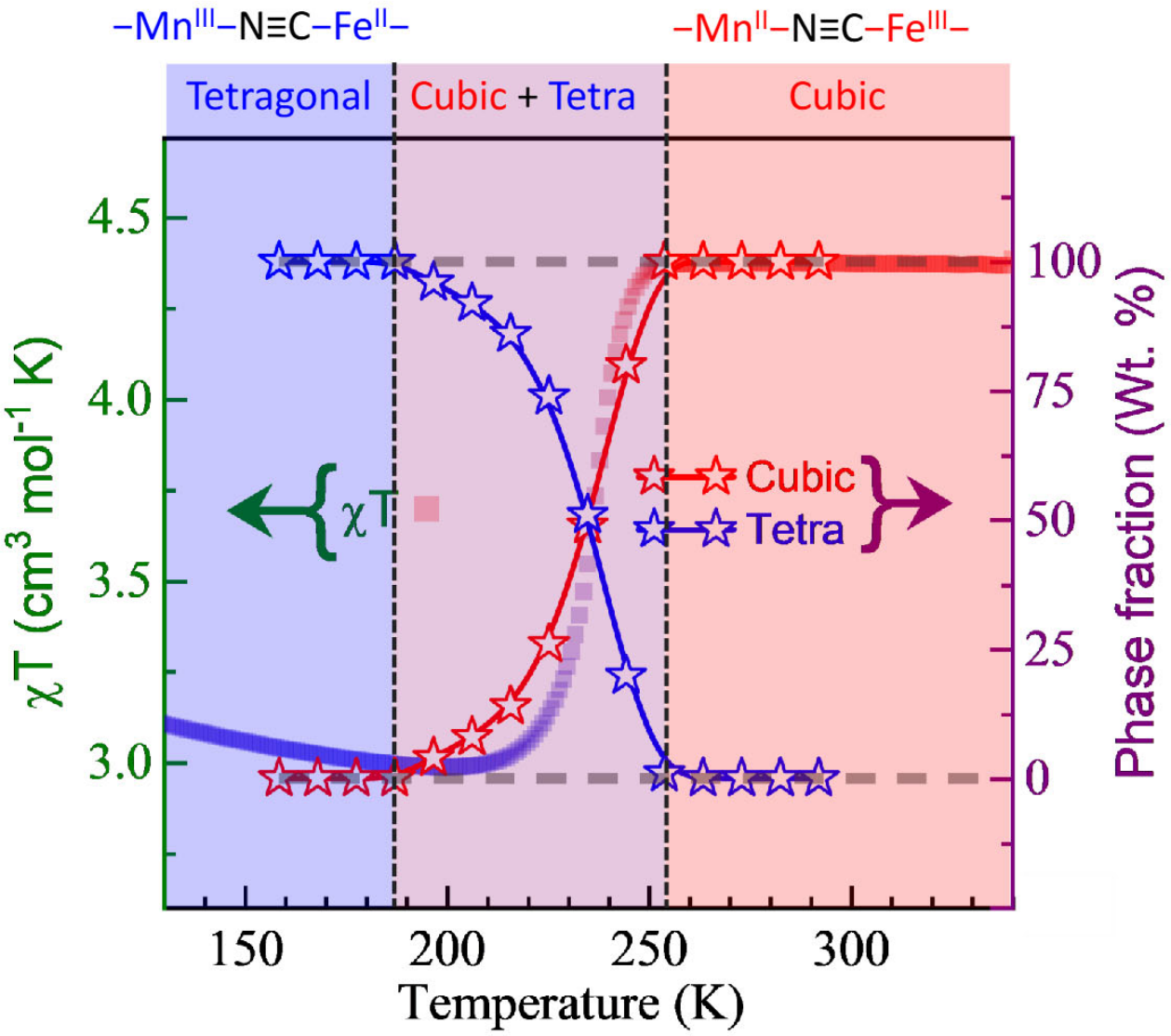

Effect of Rb content on structure and Charge-transfer transition

$Rb_{0.94}Mn[Fe(CN)_6].H_2O$

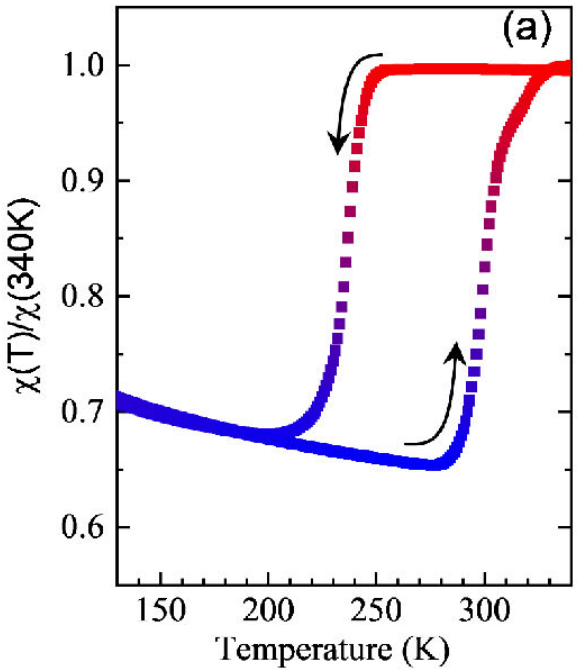

$Rb_{0.77}Mn[Fe(CN)_6]_{0.93}.1.3H_2O$

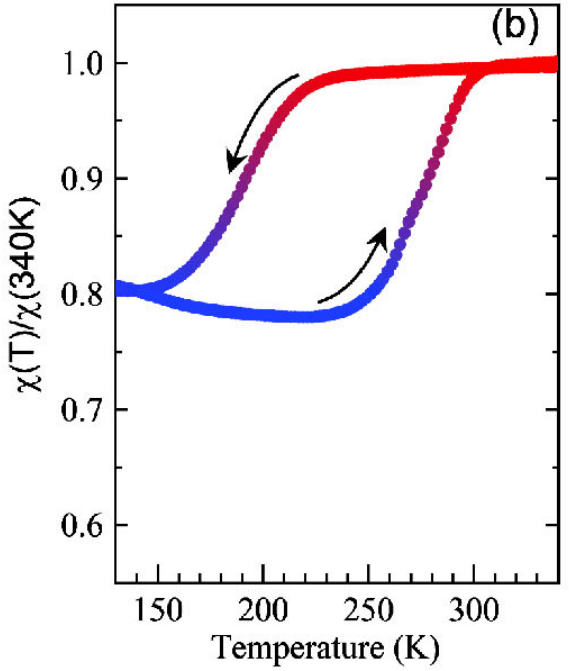

The hysteresis moved to a lower temperature

$Rb_{0.49}Mn[Fe(CN)_6]_{0.87}.2H_2O$

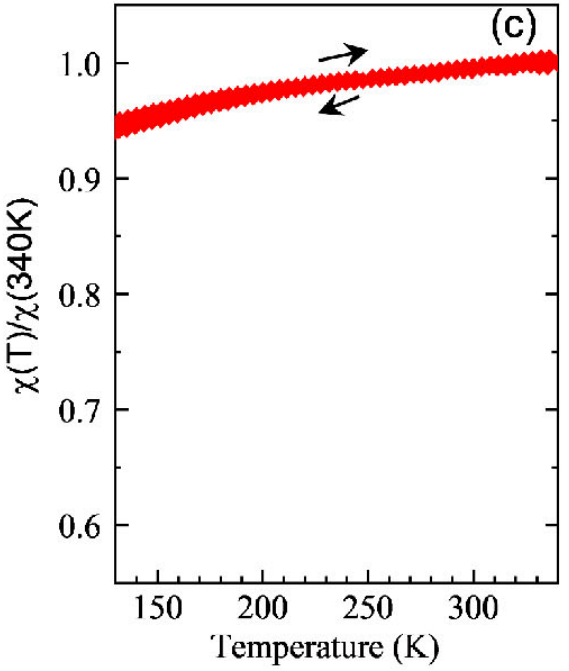

No bistability

Effect of Rb occupancy on HT structure

$Rb_{0.94}Mn[Fe(CN)_6].H_2O$

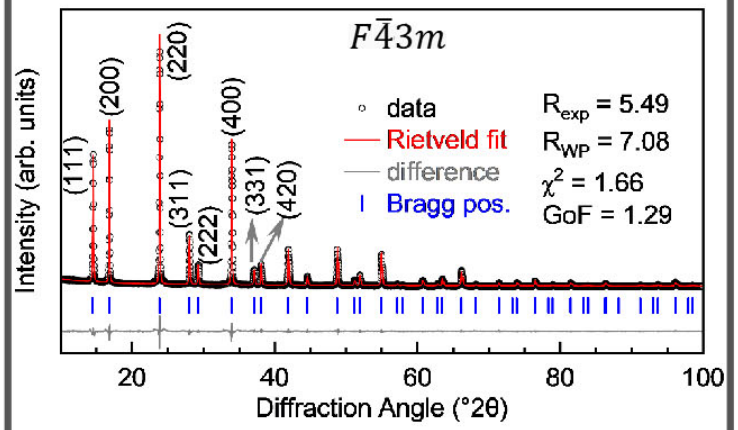

Rb (4c) (0.93)
Rb (4d) (0.01)

Rb occupies either 4c or 4d site

Lattice parameter:
a = 10.5693(5) Å

Bond lengths
Mn–N = 1.96(1) Å
Fe–C = 2.18(1) Å
C–N = 1.14(1) Å

$Rb_{0.77}Mn[Fe(CN)_6]_{0.93}.1.3H_2O$

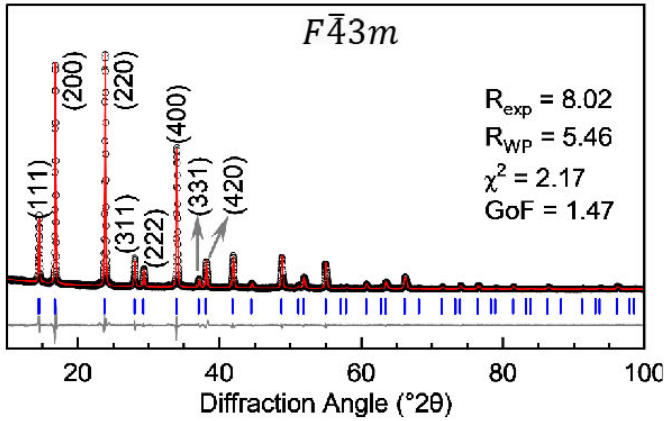

Rb (4c) (0.69)
Rb (4d) (0.08)

Rb occupation start to be random

Lattice parameter:
a = 10.5594(9) Å

Bond lengths
Mn–N = 2.06(1) Å
Fe–C = 2.09(1) Å
C–N = 1.12(1) Å

$Rb_{0.49}Mn[Fe(CN)_6]_{0.87}.2H_2O$

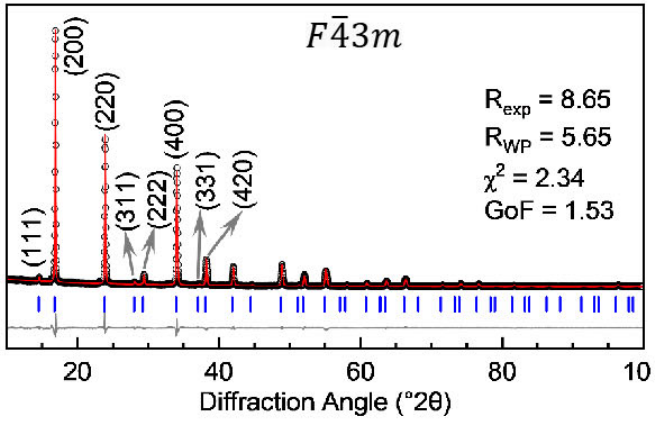

Rb (4c) (0.31)
Rb (4d) (0.18)

Rb occupation is approaching 50/50

Lattice parameter:
a = 10.5474(8) Å

Bond lengths
Mn–N = 2.13(1) Å
Fe–C = 2.00(1) Å
C–N = 1.14(1) Å

Encapsulation of microcrystals in Polyvinylpyrrolidone (PVP)

Electrospinning technique

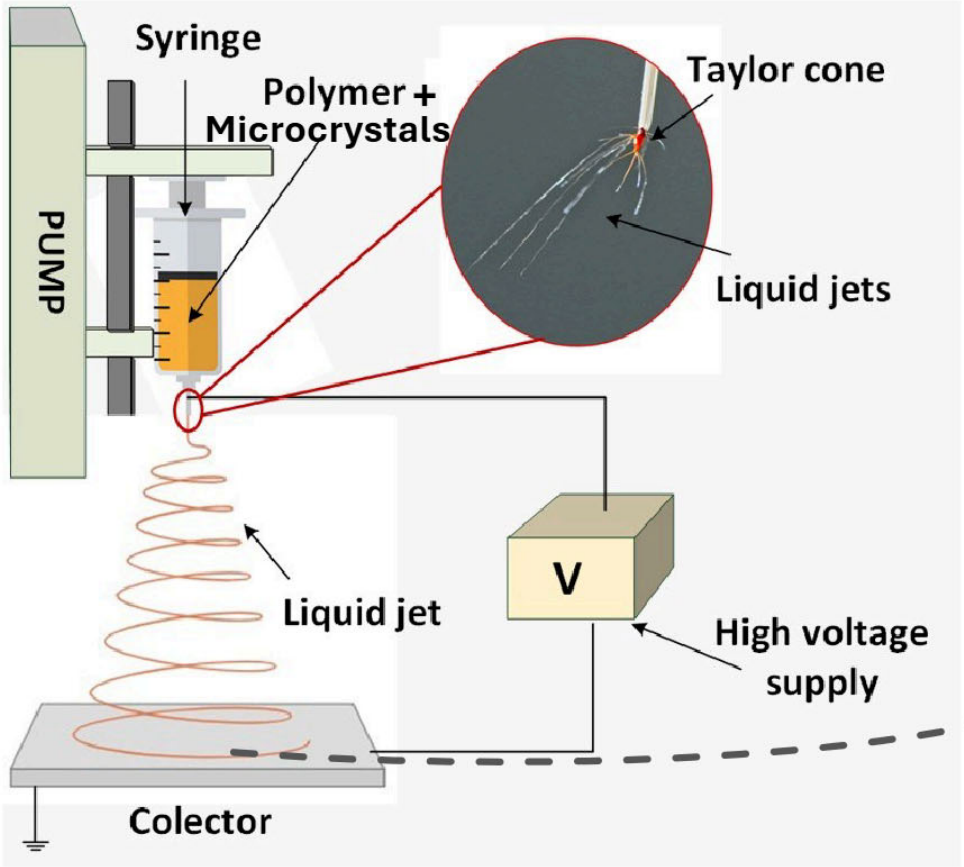

SEM: Confirms the encapsulation of microcrystals in PVP

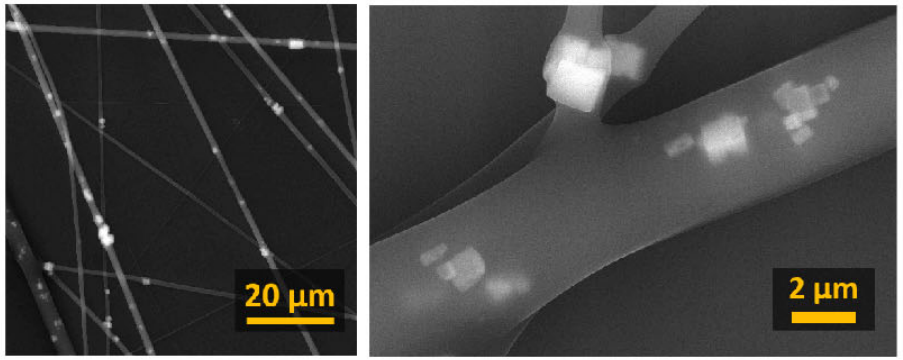

Spun-mat (composite) with ~11-12% microcrystals by weight.

Identical average structures in microcrystals and composites

Microcrystals: $Rb_{0.94}Mn[Fe(CN)_6].H_2O$

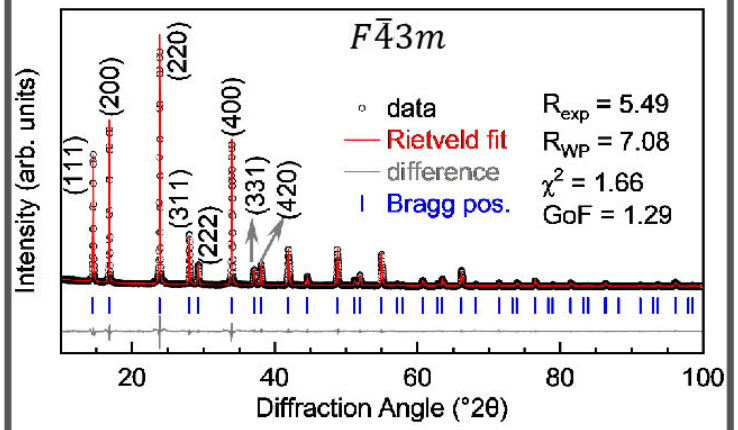

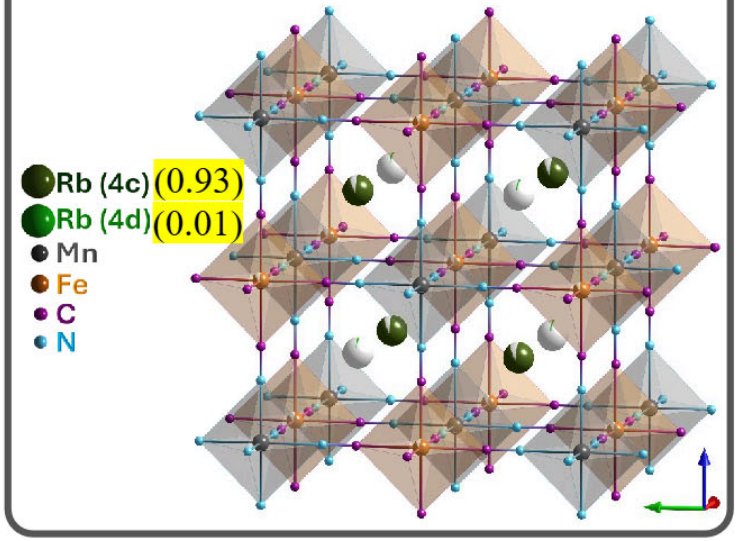

Composite: $Rb_{0.94}Mn[Fe(CN)_6].H_2O$ in PVP

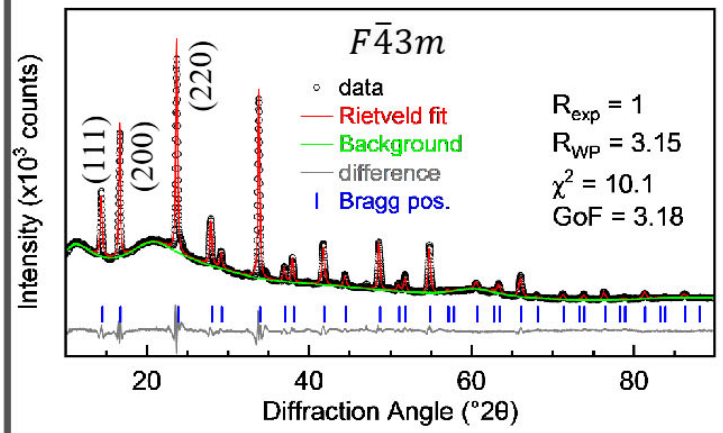

The structure parameters of polymer complexes are similar to those of microcrystals. So we can conclude that the average structures are identical.

What about the local structures in microcrystals and composites?

Microcrystals: $Rb_{0.94}Mn[Fe(CN)_6].H_2O$

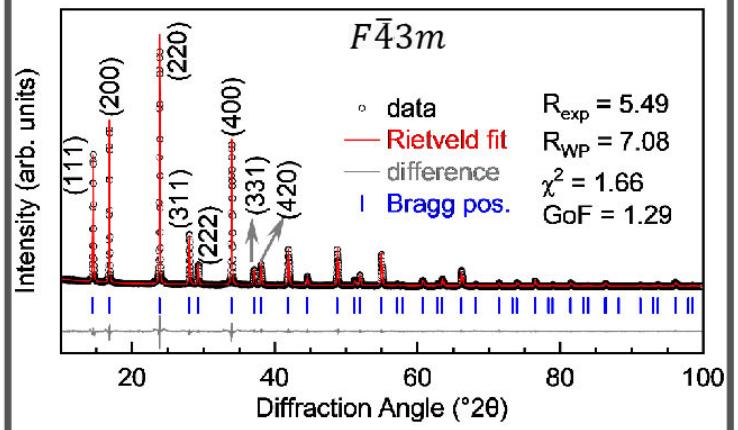

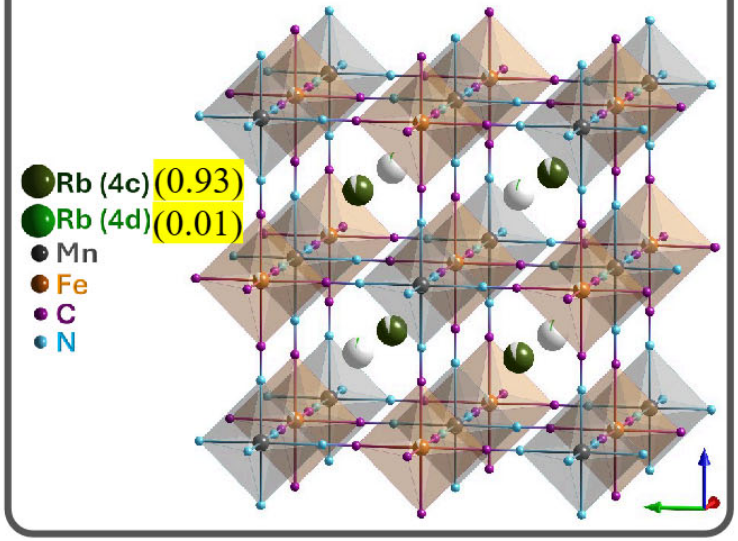

Composite: $Rb_{0.94}Mn[Fe(CN)_6].H_2O$ in PVP

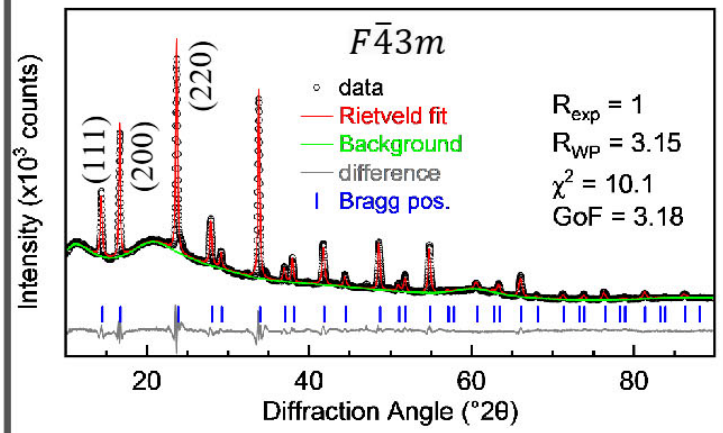

The structure parameters of polymer complexes are similar to those of microcrystals. So we can conclude that the average structures are identical.

That begs the question:

What about local structure, does the first coordination shell survive embedding?

Element-specific Mn K-edge XANES can provide the answer.

XANES Confirms Unchanged Local Structure

ASTRA @SOLARIS, Krakow

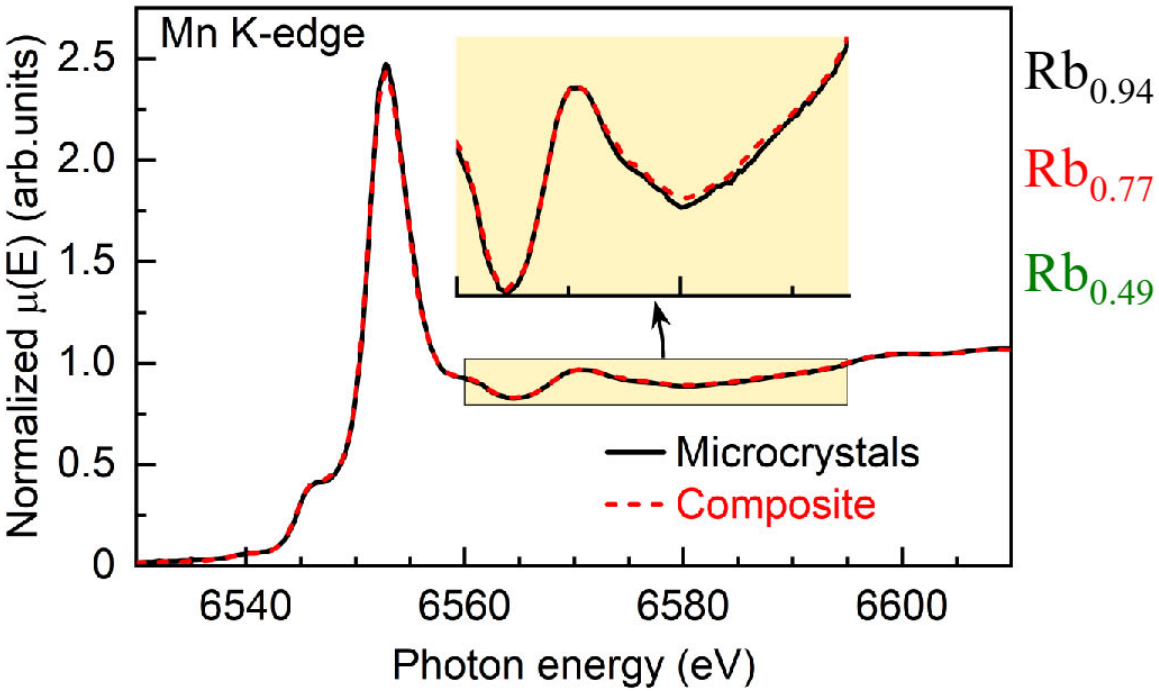

Crucially, XANES spectra for microcrystals and the composite are identical at RT, so the polymer does not chemically perturb the metal sites, and observed changes are not redox or defect-chemistry artefacts.

A. Pacanowska et al., J. Mol. Liq. **437** (2025)

Enhanced Hysteresis in Polymer–Crystal Composites

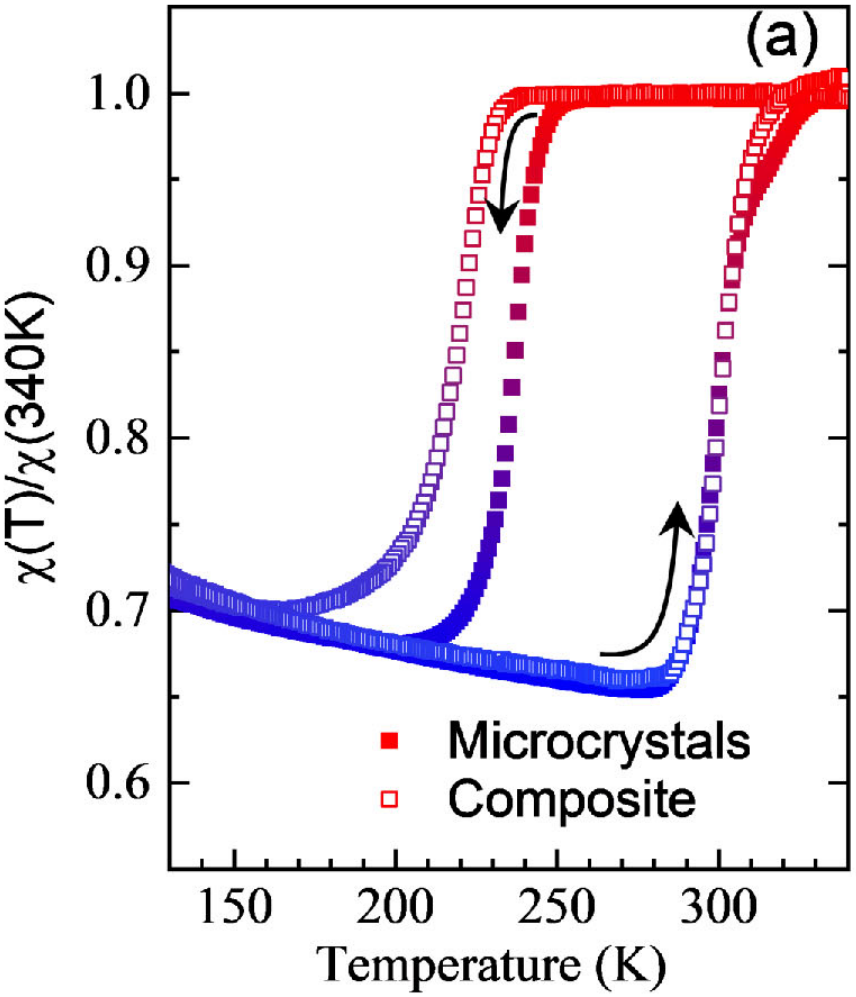

$Rb_{0.94}Mn[Fe(CN)_6].H_2O$

The thermal hysteresis of susceptibility is broader in microcrystals embedded in polymer, due to a significant shift of the HT-LT transition to lower temperatures.

What is the possible origin of wider thermal hysteresis in composites?

A. Pacanowska et al., J. Mol. Liq. **437** (2025)

Pressure-driven control of electronic and structural phases

Microcrystals under hydrostatic pressure

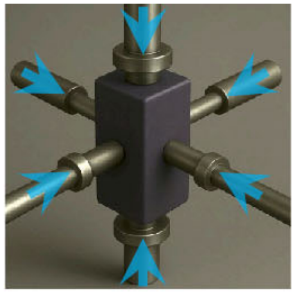

Transition temperature:

$$T_c(p) = T_{\text{ambiant}} + \Delta T$$

Compressive stress increases the transition temperatures

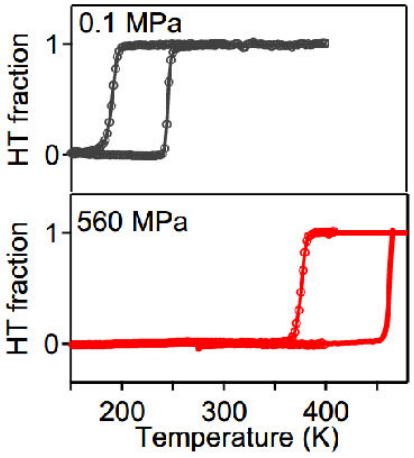

S. Ohkoshi, et. al., *Nat Commun,* **14(1)** (2023)

Microcrystals: Ambient pressure

$T > T_c$

Cooling

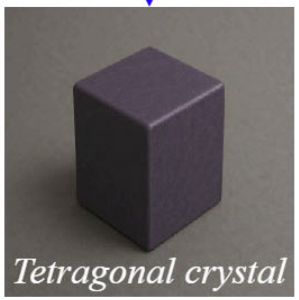

$T < T_c$

Transition temperature:

$$T_c\,(\text{p=0}) = T_{\text{ambiant}}$$

Microcrystals in polymer = Tensile pressure

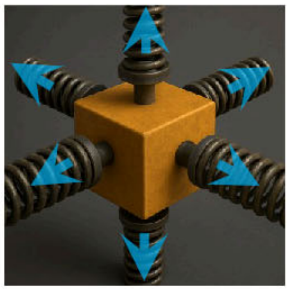

Transition temperature:

$$T_c(p) = T_{\text{ambiant}} - \Delta T$$

Tensile stress decreases the transition temperatures

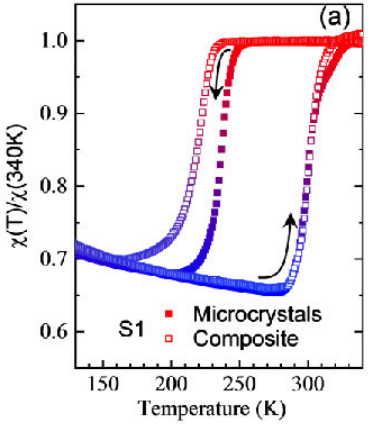

A. Pacanowska et al., J. Mol. Liq. **437** (2025)

Unresolved: microscopic nature of magnetic order at low temperatures

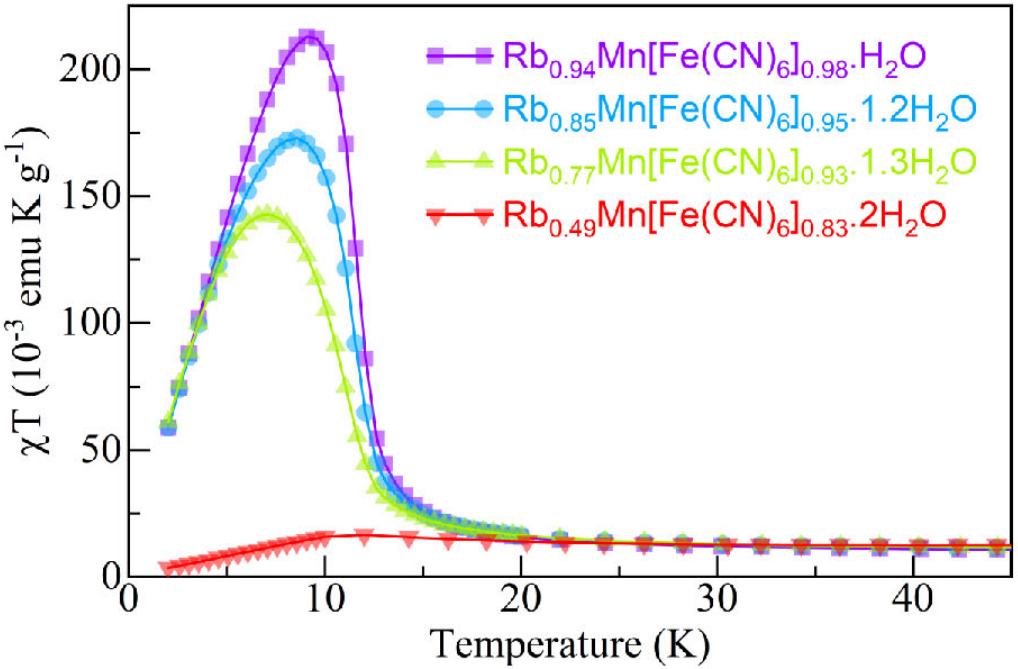

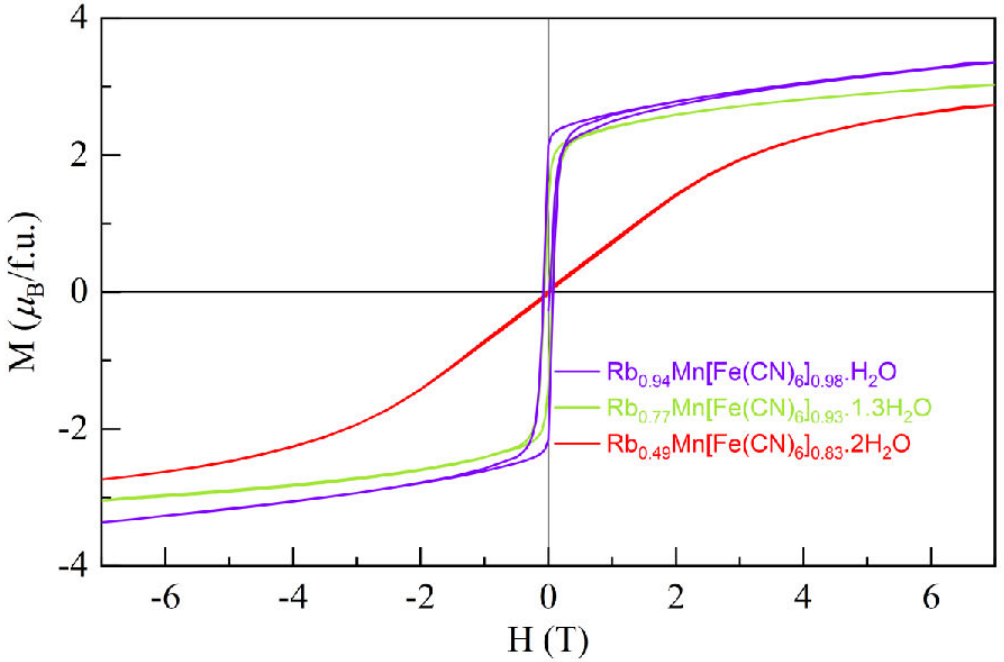

- Peak near 8–12 K reflects cooperative ordering of the Mn^{3+} sublattice.
- Amplitude decreases as $Fe(CN)_6$ vacancies break Mn^{3+}–N≡C–Fe^{2+}–C≡N–Mn^{3+} exchange bridges.
- Rb-rich samples → rapid rise + near-saturation → ferro-/canted Mn^{3+} order.
- Vacancy-rich sample → reduced moment, no saturation → exchange dilution → short-range correlations.

Sawtooth lattice multiferroic $BeCr_2O_4$

Synchrotron x-ray diffraction pattern

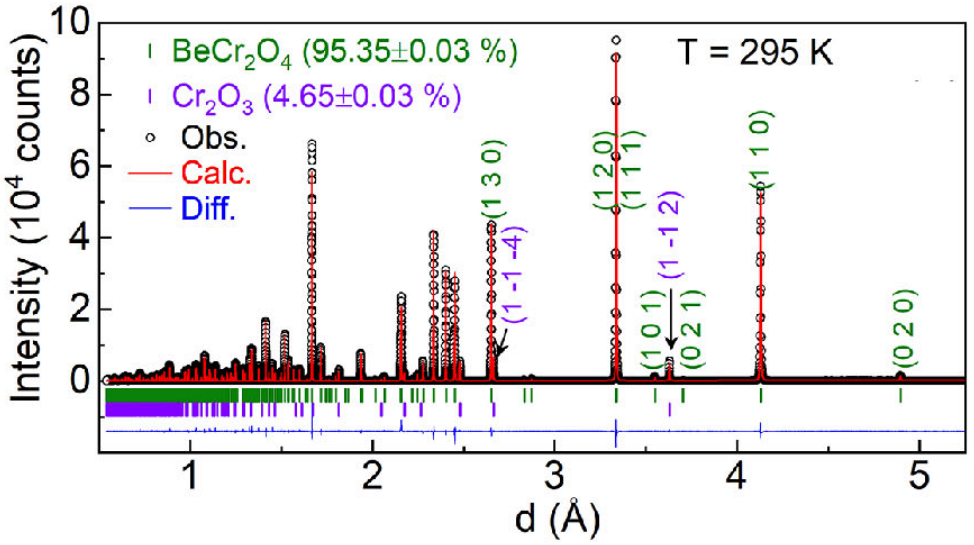

Refined structure

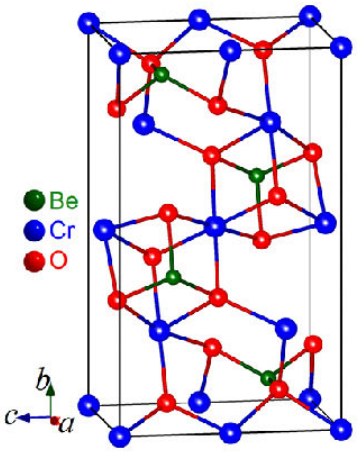

Orthorhombic *(Pbnm)*

Sawtooth lattice formed by two Cr sites

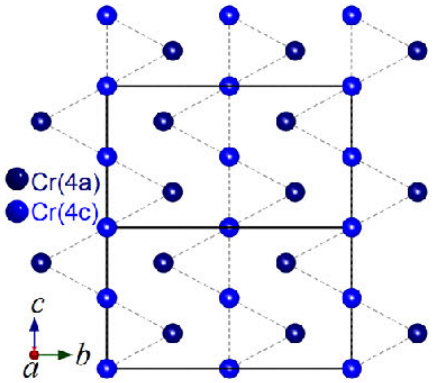

4*a* (0, 0, 0)
4*c* (*x*, *y*, 0.75)

H. C. Mandujano, CMNK *et al*., Phys. Rev. B **7**, 024422 (2023).

- One of the earliest compounds proposed to be a multiferroic.
- Polycrystalline samples were prepared using a solid-state reaction route.
- A small impurity of Cr_2O_3 was found, which could be refined and quantified.

D. E. Cox, et al, J. Appl. Phys. **40**, 1124 (1969).

- In sawtooth magnetic lattices, similar to triangular lattices, we expect multiple competing magnetic orders, including incommensurate magnetic structures, due to magnetic frustration.

Specific heat measurements indicate two anomalies

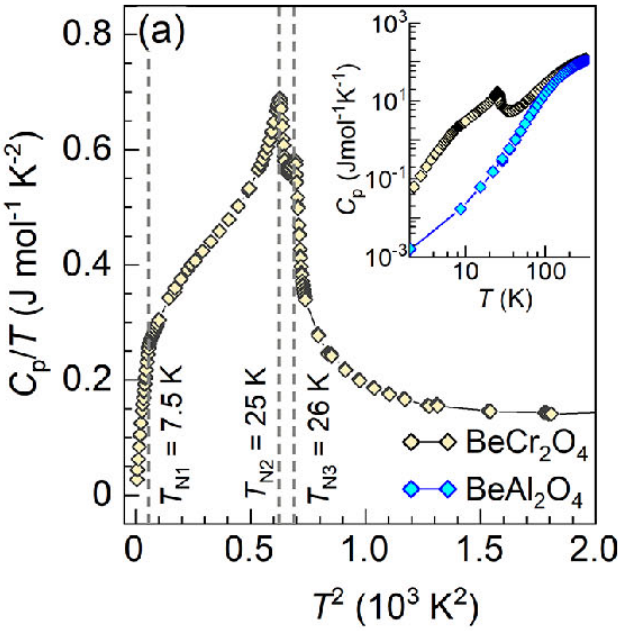

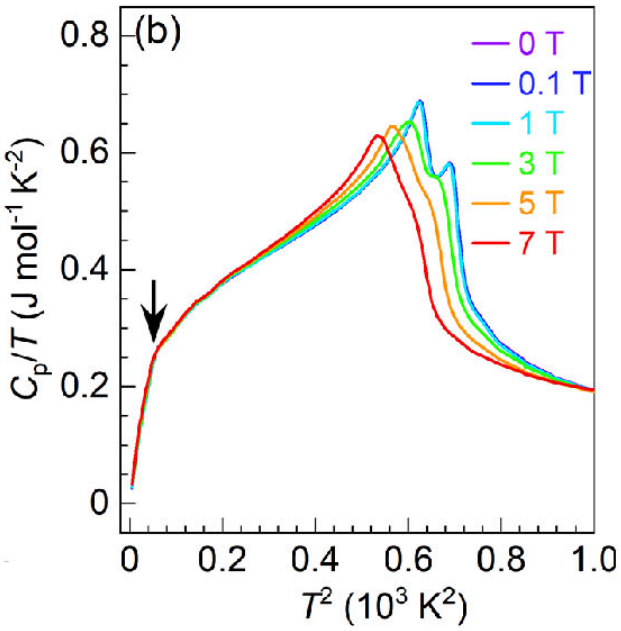

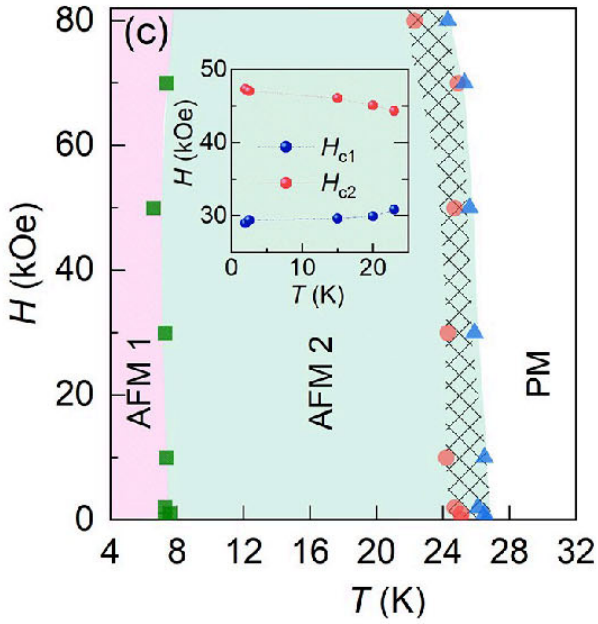

H. C. Mandujano, CMNK *et al.*, Phys. Rev. B **7**, 024422 (2023).

- Specific heat data confirm the two anomalies observed in magnetization measurements, in addition, a third anomaly is observed around 7 K.
- Based on these macroscopic measurements we were able to construct this temperature vs magnetic field phase diagram.

Magnetization confirms two magnetic transitions

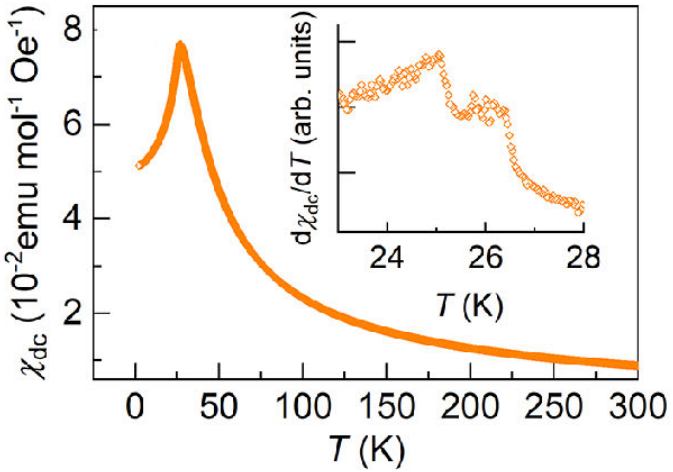

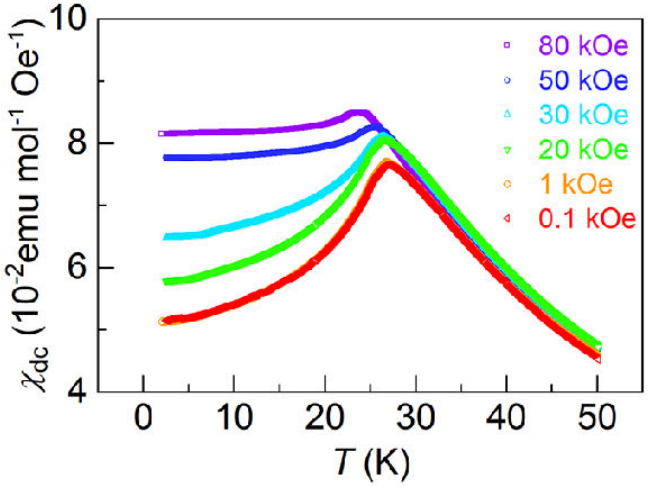

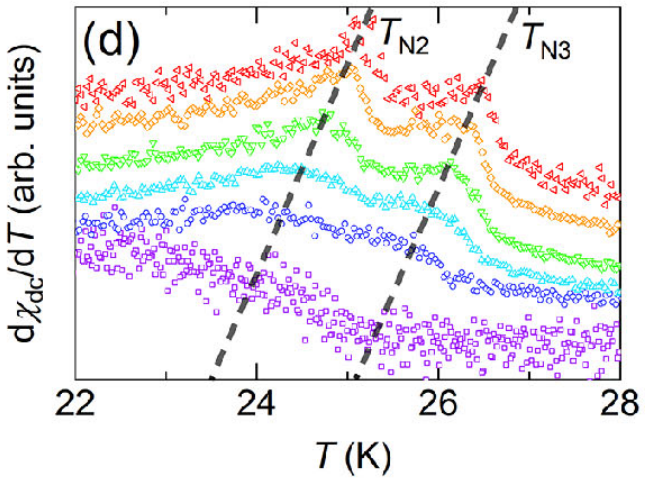

H. C. Mandujano, CMNK *et al*., Phys. Rev. B **7**, 024422 (2023).

- Two magnetic anomalies were observed in from magnetization measurements around 25 K, which evolve with the fields.

Neutron scattering measurements

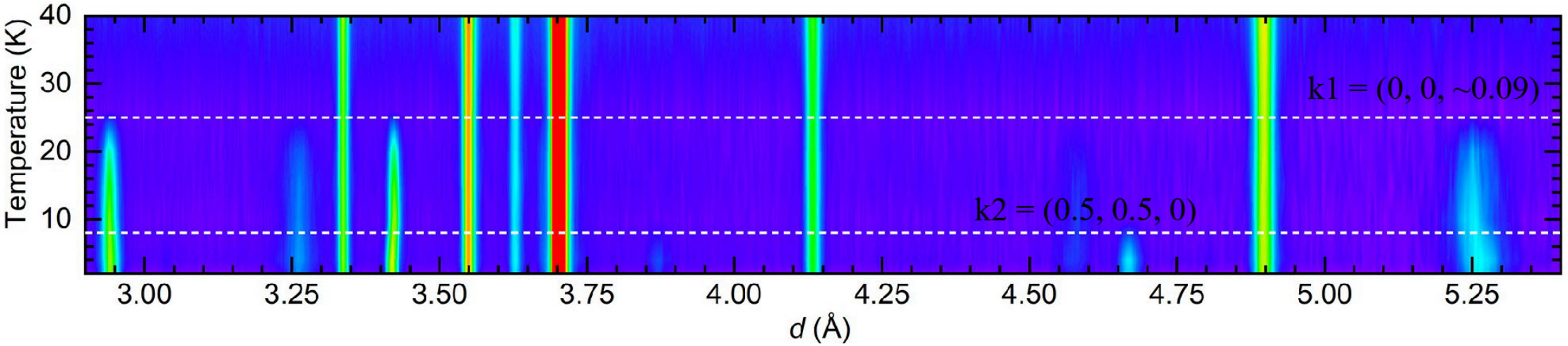

A contour map of neutron powder diffraction patterns collected at several temperatures

H. C. Mandujano, CMNK *et al*., Phys. Rev. B **7**, 024422 (2023).

- In contrast to the two anomalies observed around 25 K, in macroscopic measurements, neutron powder diffraction data showed only one anomaly characterized by the appearance of new Bragg peaks.
- Additional peaks appear around 7 K, corresponding to the third anomaly observed in heat capacity measurements.
- Keeping the parent structure to be *Pbnm,* the high-temperature satellite is found to be k_1. At low temperatures, additional satellite peaks appear, which were indexed as k_2.

Magnetic structure solutions from neutron diffraction data

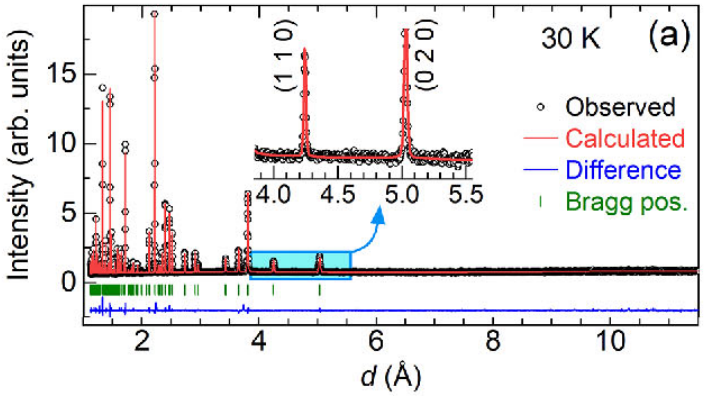

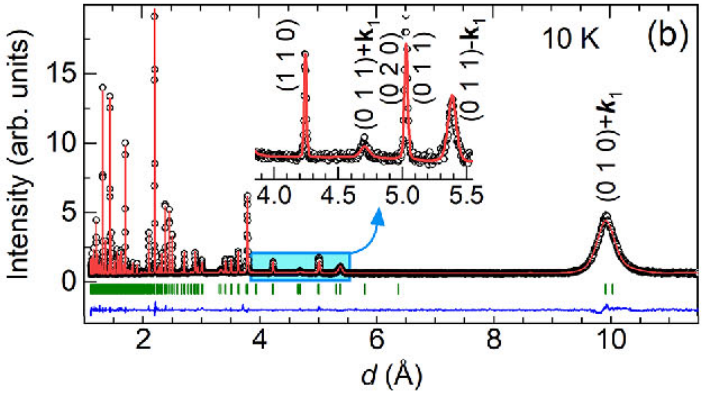

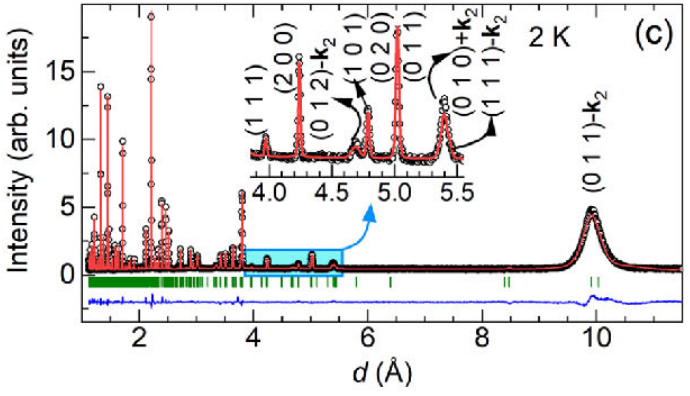

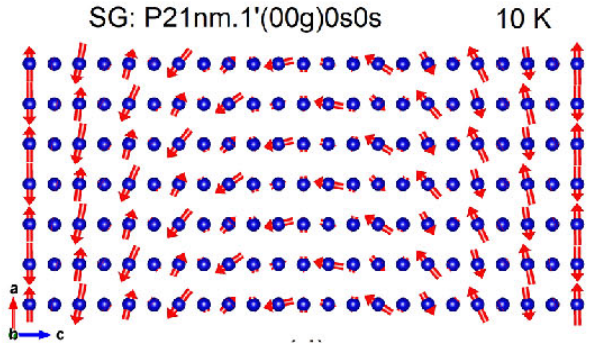

H. C. Mandujano, CMNK *et al*., Phys. Rev. B **7**, 024422 (2023).

- At 30 K (paramagnetic range), the refined structure is similar to that obtained from synchrotron X-ray data.
- In the temperature range ~7 - 25 K ($T_{N1} < T < T_{N2}$), the magnetic structure is found to be a cycloid with an incommensurate magnetic wave vector $\mathbf{k}_1$ = (0 0 0.092(1)) plus a commensurate (0.5 0.5 0). This structure will induce ferroelectric polarization along the crystallographic *a* - direction.
- Below 7 K ($T < T_{N1}$), the magnetic structure is incommensurate with a new propagation vector $\mathbf{k}_2$ = (0 0 0 0.908(1)).
- The magnetic order in the temperature range $T_{N2}<T_{N3}$ (~1 K range) could not be resolved from powder diffraction data.

Using ESS: Instruments & Motivation

- The possibility to measure neutron scattering on sub-milligram crystals is necessary to resolve the structures as a function of temperature with greater temperature precision.

ESS uniquely enables these measurements due to its high brilliance and low background — essential for weak magnetic signals or sub-milligram samples.

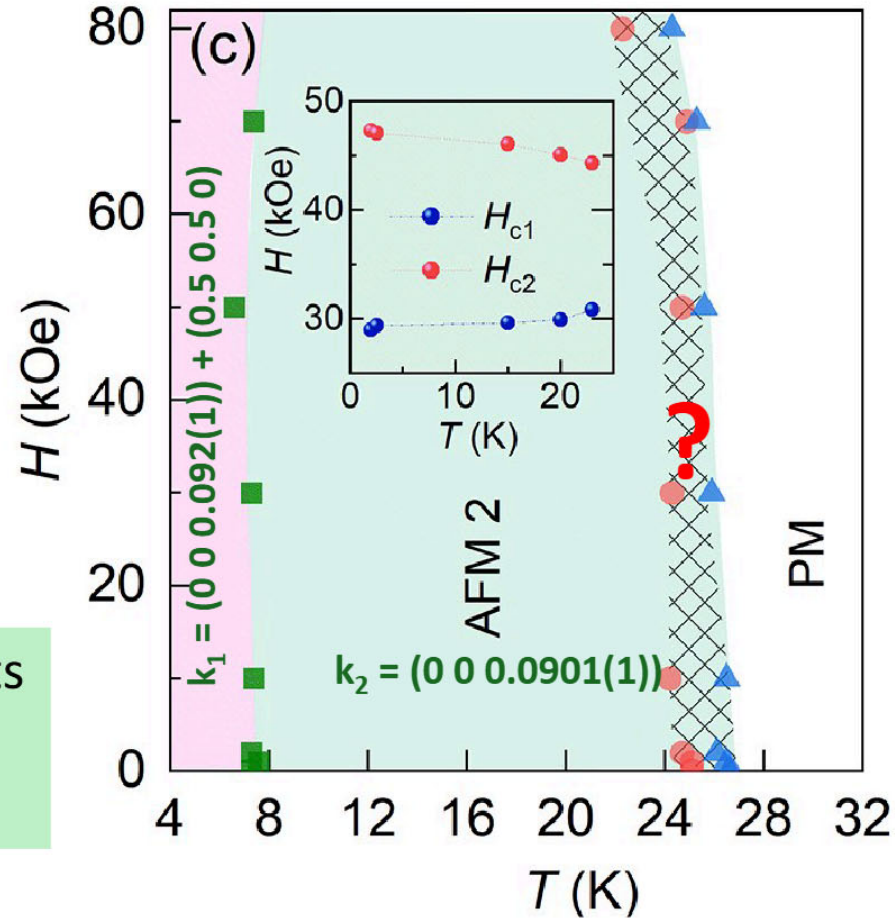

ESS Opportunities for Molecular Magnets & Frustrated Oxides

• **Structural responses to external stimuli**
– **DREAM / BEER**: high-resolution diffraction on milligram-scale samples to follow lattice changes under **temperature, pressure, hydration, and E-fields**. It can resolve magnetic order, moment size, vacancy effects, complex AFM / noncollinear order, and magnetoelastic coupling.

• **Mixed-valence and low-energy excitations**
–**CSPEC**: probe **spin, orbital, and charge-transfer excitations**, Jahn–Teller modes, coupling pathways, exchange energies, spin-wave spectra, frustration-driven excitations.

• **Vacancy and hydration effects**
– **HEIMDAL**: combined diffraction + SANS to map **vacancy ordering**, **short-range correlations**, **water-dependent structural disorder**, frustrated correlations, partial order, and spin-cluster signatures.

• **BEER / High-Pressure Options**
– Structural & magnetic transitions under pressure or field in both systems.

ESS Advantage
High flux + low background → full static and dynamic information from sub-mg samples and weakly scattering magnets.